The Astrophysical Journal Letters, 783:L27 (4pp), 2014 March 10 doi:10.1088/2041-8205/783/2/L27

ANISOTROPIC INTERMITTENCY OF MAGNETOHYDRODYNAMIC TURBULENCE

K. T. Osman[1], K. H. Kiyani[1,2], S. C. Chapman[1,3,4], and B. Hnat[1]
[1] Centre for Fusion, Space and Astrophysics, University of Warwick, Coventry CV4 7AL, UK; k.t.osman@warwick.ac.uk
[2] Laboratoire de Physique des Plasmas, École Polytechnique, Route de Saclay, F-91128 Palaiseau, France
[3] Department of Mathematics and Statistics, University of Tromsø, NO-9037 Tromsø, Norway
[4] Max Planck Institute for the Physics of Complex Systems, D-01187 Dresden, Germany
Received 2014 January 4; accepted 2014 January 31; published 2014 February 24

ABSTRACT

A higher-order multiscale analysis of spatial anisotropy in inertial range magnetohydrodynamic turbulence is presented using measurements from the *STEREO* spacecraft in fast ambient solar wind. We show for the first time that, when measuring parallel to the local magnetic field direction, the full statistical signature of the magnetic and Elsässer field fluctuations is that of a non-Gaussian globally scale-invariant process. This is distinct from the classic multiexponent statistics observed when the local magnetic field is perpendicular to the flow direction. These observations are interpreted as evidence for the weakness, or absence, of a parallel magnetofluid turbulence energy cascade. As such, these results present strong observational constraints on the statistical nature of intermittency in turbulent plasmas.

Key words: magnetohydrodynamics (MHD) – plasmas – solar wind – turbulence

Online-only material: color figures

1. INTRODUCTION

Turbulence is a universal fluid phenomenon that generates intermittent fluctuations (Bruno & Carbone 2013). The solar wind provides an ideal laboratory for the in situ study of plasma turbulence, wherein intermittent fluctuations have been analyzed in considerable detail. These have been linked to non-uniform plasma heating (Osman et al. 2011a, 2012b; Wu et al. 2013) and enhanced turbulent dissipation (Wan et al. 2012; Karimabadi et al. 2013; TenBarge & Howes 2013). In addition, there is evidence to suggest that increased alpha particle (Perrone et al. 2013), proton (Servidio et al. 2012), and electron (Haynes et al. 2014) temperature anisotropies are associated with intermittent structures. The same structures can cause particle velocity distribution functions to deviate from local thermal equilibrium (Greco et al. 2012) and have been preferentially found in plasma unstable to microinstabilities (Osman et al. 2012a). A subset of non-Gaussian intermittent structures correspond to active magnetic reconnection sites (Servidio et al. 2011) which can in turn generate fluctuations that exhibit the hallmarks of intermittency (Leonardis et al. 2013). These spatial structures may also be related to trapping boundaries that delineate dropouts of energetic particle flux as seen in solar energetic particle data (Ruffolo et al. 2003). Indeed, recent work suggests that these structures contribute to the acceleration and transport of interplanetary suprathermal particles (Tessein et al. 2013). Intermittent fluctuations are the reason why turbulence can enhance the transport of particles, heat, momentum, and current in laboratory plasmas. The intermittent structures in plasmas share striking similarities with fluctuations found in turbulent neutral fluids (Frisch 1995; Sreenivasan & Antonia 1997). Therefore, quantifying intermittency is central to understanding and interpreting a large body of observations in turbulent systems.

Intermittency lies at the heart of turbulence theory. The classical signatures of intermittency in both neutral fluid and magnetohydrodynamic (MHD) turbulence are a non-Gaussian probability distribution function (PDF) of fluctuations and multifractal scaling in the higher-order statistics (Bruno & Carbone 2013). However, non-fluid phenomenology such as the kinetic range of plasma turbulence can have a monofractal scaling (Kiyani et al. 2009). These different scaling types imply different underlying physics. We will quantify both the non-Gaussian behavior of fluctuations and their statistical scaling in the turbulent solar wind. Intermittency is related to the emergence of small-scale coherent structures that are responsible for enhanced dissipation. Hence, the most fundamental approach to the study of intermittency is to examine the dissipation rate PDF. However, the Kolmogorov refined similarity hypothesis (hereafter KRSH; Kolmogorov 1962; Oboukhov 1962) allows local averages of the dissipation rate to be related to increments of the velocity field calculated on different spatial scales, r. The PDF of velocity increments is then linked to intermittency (Anselmet et al. 1984), where departures from a normal distribution occur on small spatial scales while large-scale features are uncorrelated and converge toward a Gaussian distribution. This non-Gaussian behavior is also observed in the turbulent solar wind magnetic field (Sorriso-Valvo et al. 1999). A method to quantify intermittency is based on computing a sequence of mth order moments of the magnetic or velocity field increments. For an increment scale r, the moments have power-law scalings, $\propto r^{\zeta}$, where the exponents ζ depend on the moment order m. Here the physical meaning lies in the sensitivity of higher-order moments to concentrations of dissipation and, from KRSH, to large increments. The behavior of these exponents is also connected to known fractal and multifractal models (Frisch et al. 1978; She & Leveque 1994; Politano & Pouquet 1995). This Letter presents novel observational results from a higher-order analysis that examines the statistical properties of MHD turbulence in the spatially anisotropic solar wind. We find for the first time that these statistical properties depend on the angle of the local magnetic field direction to the (radial) solar wind flow. This provides strong constraints on the physics and phenomenology of inertial range turbulence in collisionless plasmas.

The presence of a magnetic field in plasma turbulence breaks the isotropy found in hydrodynamics and orders the fluctuations (Horbury et al. 2005). In the solar wind, fluctuation components parallel and transverse to the background magnetic field display differences in dynamics and statistics (Chapman

Table 1
List of all the High-speed Streams in the Ecliptic Plane that are Analyzed

No.	Year	[UT] Start	[UT] End	Days	S/C
1	2007	Apr 28 00:00	May 1 00:00	3	STB
2	2007	May 25 00:00	May 28 02:39	3.11	STB
3	2007	Aug 27 12:00	Aug 30 12:00	3	STB
4	2007	Nov 15 00:00	Nov 18 00:00	3	STA
5	2008	Jan 8 00:00	Jan 11 00:00	3	STA
6	2008	Feb 13 00:00	Feb 18 00:00	5	STA
7	2008	Mar 8 00:00	Mar 11 00:00	3	STB
8	2008	Apr 4 00:00	Apr 8 00:00	4	STB
9	2008	May 2 12:00	May 6 00:00	3.5	STB

Note. Here S/C represents spacecraft, where STA is *STEREO* A and STB is *STEREO* B.

& Hnat 2007). However, this "variance" anisotropy is not reflected in the higher-order moments and both components display a multifractal intermittent scaling (Kiyani et al. 2013). The distribution of energy over the full three-dimensional (3D) space of wavevectors is also anisotropic (Oughton et al. 1994). This spatial anisotropy has been observed in second-order statistics such as the power spectral density (PSD; Osman & Horbury 2009b) and correlation function (Matthaeus et al. 1990; Osman & Horbury 2007, 2009a). It has also been found in third-order statistics (Osman et al. 2011b). A higher-order analysis of wavevector anisotropy would provide a direct test of theoretical predictions regarding the statistical nature of intermittency and, more broadly, the phenomenology of the turbulent cascade. However, an investigation into the wavevector anisotropy of intermittent fluctuations has not, to the best of our knowledge, been conducted.

2. ANALYSIS

We use 8 Hz magnetic field measurements from the IMPACT instrument (Acuña et al. 2008; Luhmann et al. 2008) and 1 minute resolution proton plasma data from the PLASTIC instrument (Galvin et al. 2008) on board the two *STEREO* spacecraft in the ecliptic. The solar wind intervals used here are all in high-speed streams and contain no sector crossings. These are listed in Table 1 and are identical to those used by Podesta (2009). It has been suggested (e.g., Chapman & Hnat 2007; Horbury et al. 2008) that a local scale-dependent mean magnetic field and associated scale-dependent fluctuations, rather than a large-scale global field (Matthaeus et al. 2012), should be used in anisotropy studies of plasma turbulence. Hence, we use the undecimated discrete wavelet transform method described in Kiyani et al. (2013) to decompose the magnetic field into a local scale-dependent background and fluctuations, $\bar{\mathbf{B}}(t, f)$ and $\delta\mathbf{B}(t, f)$, where f explicitly shows the frequency or scale dependence. These fluctuations are binned according to the angle of the local magnetic field direction to the (radial) flow, θ_{VB}. Here we focus on fluctuations in the $\theta_{VB} = 0°$–$10°$ and $80°$–$90°$ bins, which correspond to wavenumbers using Taylor's hypothesis (Taylor 1938) that are, respectively, nearly field-parallel $\delta\mathbf{B}(k_\parallel)$ and nearly field-perpendicular $\delta\mathbf{B}(k_\perp)$.

3. RESULTS

We present a detailed analysis of interval eight listed in Table 1, which is typical of the stationary fast solar wind intervals used in this study. The PSD is independent of the azimuthal angle about the local magnetic field for all relevant spacecraft frame frequencies (Podesta 2009). Hence, the spacecraft frame wavelet PSD depends only on the angle of the magnetic field to the flow direction:

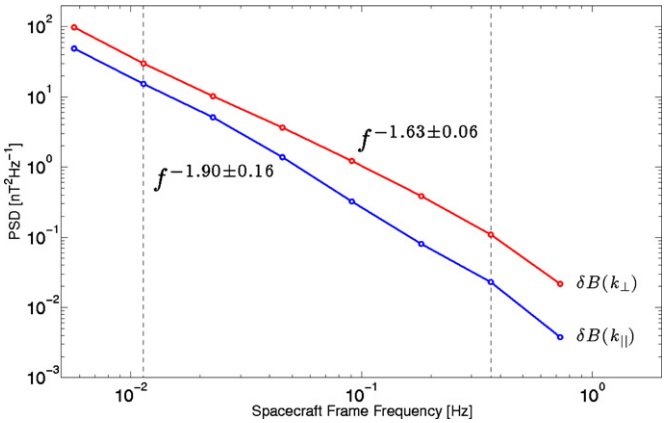

Figure 1. PSD of the trace magnetic field fluctuations for the angular bins $\theta_{VB} = 0°$–$10°$ (squares) and $80°$–$90°$ (circles). The power-law spectral index α for each PSD is shown alongside the data in the form $f^{-\alpha}$.
(A color version of this figure is available in the online journal.)

$$\mathrm{PSD}(f, \theta_{VB}) = \frac{2\Delta}{N}\sum_{j=1}^{N}\delta B^2(t_j, f, \theta_{VB}), \quad (1)$$

where $\delta B(t_j, f, \theta_{VB})$ is the magnitude of the trace fluctuations at time t_j and frequency f, Δ is the sampling time between consecutive measurements, and N is the sample size at each frequency. Figure 1 shows the PSD for two angular bins, $\theta_{VB} = 0°$–$10°$ and $80°$–$90°$, which correspond to wavevectors roughly parallel and perpendicular to the local field, respectively. These are both well described by power laws. The power levels are lower and the spectral slope is steeper for $\delta\mathbf{B}(k_\parallel)$ compared to $\delta\mathbf{B}(k_\perp)$, which is consistent with previous studies (e.g., Horbury et al. 2008; Podesta 2009). Hence, the statistical behavior of fluctuations in wavevectors at large angles to the magnetic field would have dominated all previous estimates of the inertial range intermittency, since these contain the most power. The dashed vertical lines define the typical range of timescales used in the higher-order analysis. However, this range of timescales is varied slightly for each higher-order analysis in order to minimize the errors associated with the computed scaling exponents.

In order to determine the higher-order scaling of fluctuations for different θ_{VB}, we compute the absolute moments of the magnetic field increments, $\delta B(t, \tau) = B(t + \tau) - B(t)$. The mth order wavelet structure function is given by

$$S^m(\tau, \theta_{VB}) = \frac{1}{N}\sum_{j=1}^{N}\left|\frac{\delta B(t_j, \tau, \theta_{VB})}{\sqrt{\tau}}\right|^m, \quad (2)$$

where $\tau = 2^i\Delta : i = \{0, 1, 2, 3, \ldots\}$ is the dyadic timescale parameter related to the central frequency f. Note that wavelets change the regular expressions for structure functions (Kiyani et al. 2013). The higher-order structure functions increasingly capture the more intermittent fluctuations. In hydrodynamics, these large fluctuations represent the spatial gradients responsible for dissipating the turbulent cascade energy. However, there is growing evidence to suggest these intermittent structures are also associated with non-uniform heating (Osman et al. 2011a,

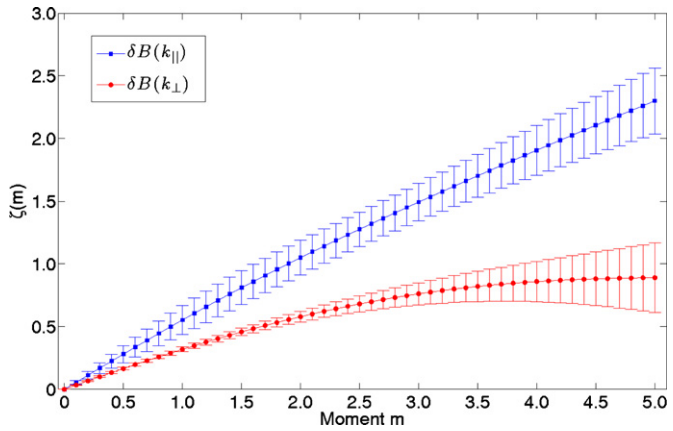

Figure 2. Scaling exponents $\zeta(m)$ for the trace magnetic field fluctuations. For fluctuations with $\theta_{VB} = 0°$–$10°$, there is a linear relationship on this plot that indicates fractal scaling. There is a distinct nonlinear (concave) behavior for fluctuations with $\theta_{VB} = 80°$–$90°$, which indicates a multifractal.

(A color version of this figure is available in the online journal.)

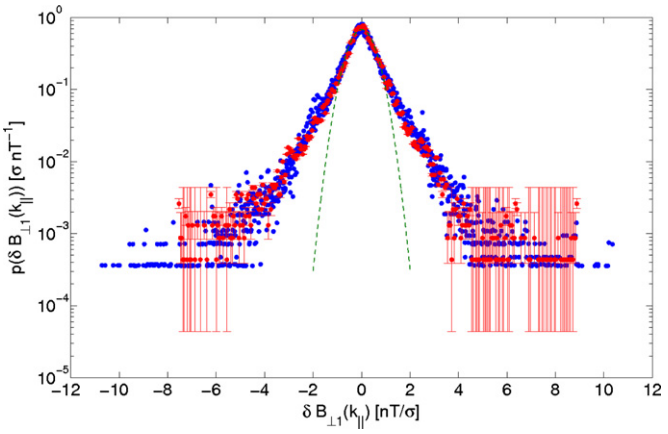

Figure 3. PDFs of the $\theta_{VB} = 0°$–$10°$ trace magnetic field fluctuations rescaled using $P_s(\delta B\sigma^{-1}) = \sigma P(\delta B, \tau)$. A Gaussian fit applied to the data (dashed curve) illustrates the heavy-tailed non-Gaussian nature of the rescaled PDF.

(A color version of this figure is available in the online journal.)

2012b; Wu et al. 2013) and increased temperature anisotropy (Servidio et al. 2012; Osman et al. 2012a; Karimabadi et al. 2013) in plasma turbulence.

Here the focus will be on the scaling behavior of structure functions, where scale invariance is indicated by

$$S^m(\tau) \propto \tau^{\zeta(m)} \tag{3}$$

and $\zeta(m)$ are the scaling exponents. Figure 2 shows the scaling exponents for both the $\theta_{VB} = 0°$–$10°$ and $80°$–$90°$ angular bins. When Equation (3) is satisfied, $\zeta(2)$ is directly related to the spectral index α by $\zeta(2) = \alpha - 1$ (Monin & Yaglom 1975). Here $\alpha(\theta_{VB} = 0°\text{–}10°) = 2.05 \pm 0.14$ and $\alpha(\theta_{VB} = 80°\text{–}90°) = 1.58 \pm 0.04$, which are consistent with the spectral indices obtained in Figure 1 from the slope of the PSD. The higher-order scaling of the magnetic field-parallel and -perpendicular fluctuations are distinct; this is a novel result. The $\theta_{VB} = 80°$–$90°$ fluctuations have a nonlinear $\zeta(m)$ that indicates a multiexponent scaling, which is characteristic of hydrodynamic turbulence (Frisch 1995) and solar wind turbulence at MHD scales (Bruno & Carbone 2013). In contrast, the $\theta_{VB} = 0°$–$10°$ fluctuations are characterized by a linear $\zeta(m) = Hm$ with a single exponent H, which indicates monoscaling. The errors on $\zeta(m)$ shown in Figure 2 were obtained from the sum of the regression error when using Equation (3), and from variations in $\zeta(m)$ that resulted from repeating the same regression over a subinterval of the original scaling range (Kiyani et al. 2006). The scaling range for the $\theta_{VB} = 0°$–$10°$ and $80°$–$90°$ fluctuations are nearly identical, but were selected independently to minimize the errors on $\zeta(m)$. In order to confirm the robustness of this result, the analysis was repeated for all nine intervals listed in Table 1 and the same θ_{VB} dependent intermittency was obtained.

The statistical analysis is completed by examining scale-by-scale the PDF for the $\theta_{VB} = 0°$–$10°$ fluctuations. A component of the trace magnetic field fluctuations is selected in order to show any symmetric or asymmetric behavior in the fluctuations. Here we use one of the components transverse to the local field, although the behavior is identical for all three vector components of the fluctuations. Since global scale invariance of the structure functions implies that the PDF of the increments at a scale τ should collapse onto a unique scaling function P_s, we use the self-affine scaling operation $P_s(\delta B\sigma^{-1}) = \sigma P(\delta B, \tau)$ to rescale the fluctuations by their standard deviation. Figure 3 shows

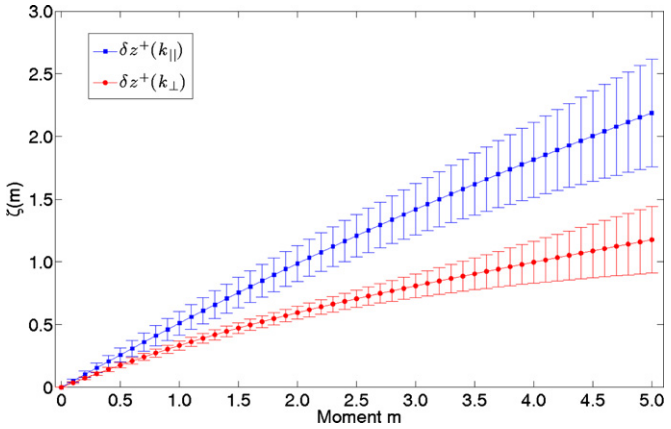

Figure 4. Scaling exponents $\zeta(m)$ for the trace anti-Sunward Elsässer field fluctuations. For fluctuations with $\theta_{VB} = 0°$–$10°$, there is a linear relationship on this plot that indicates fractal scaling. There is a distinct nonlinear (concave) behavior for fluctuations with $\theta_{VB} = 80°$–$90°$, which indicates a multifractal scaling. This anisotropic scaling is identical to that observed with the magnetic field fluctuations in Figure 2.

(A color version of this figure is available in the online journal.)

PDFs corresponding to $\tau = \{2, 4, 8, 16, 32\}$ s that are rescaled and overlaid, where the central τ is plotted in red and shows the associated errors on the PDFs. There is an excellent collapse onto a single curve, although the largest events in the tails of the distribution are not statistically well-sampled as indicated by the large errors, which is an unavoidable consequence of heavy-tailed distributions. In addition, a fitted Gaussian distribution illustrates the highly non-Gaussian nature of the PDF tails and reflects the presence of rare large amplitude fluctuations.

While the higher-order analysis has focused exclusively on magnetic field fluctuations, it is the total energy (magnetic and velocity) that is cascaded from large to small scales by plasma turbulence. Therefore, it is instructive to examine Elsässer fluctuations, $\delta\mathbf{z}^{\pm} = \delta\mathbf{V} \pm \delta\mathbf{B}$, since dynamic couplings produce structure in both magnetic and velocity fields. Here the magnetic field has been normalized to Alfvén velocity units, $\delta\mathbf{B}/\sqrt{\mu_0 m_p n_p}$, and the fluctuations have been sector rectified such that $\delta\mathbf{z}^-$ is Sunward and $\delta\mathbf{z}^+$ is anti-Sunward. Figure 4 shows the scaling exponents for the anti-Sunward Elsässer variable in both the $\theta_{VB} = 0°$–$10°$ and $80°$–$90°$ angular bins. The higher-order scaling of the fluctuations in both these bins is

similar to those in Figure 2 for the magnetic field fluctuations. The $\theta_{VB} = 80^\circ$–90° Elsässer fluctuations have a nonlinear $\zeta(m)$, which is typical of MHD scale solar wind turbulence. This behavior is also associated with the energy dissipation intensity being distributed on a spatial multifractal (Bruno & Carbone 2013). The $\theta_{VB} = 0^\circ$–10° fluctuations have a linear $\zeta(m)$, which is characteristic of global scale invariance. In theories of turbulence, this scaling behavior is associated with the energy dissipation intensity being distributed on a fractal. This analysis was repeated for the Sunward and anti-Sunward Elsässer fluctuations in all nine intervals listed in Table 1 and the same θ_{VB} dependent intermittent scaling was obtained. However, the Sunward fluctuations have greater associated errors since these are a minority and contain the least power (Gogoberidze et al. 2012).

4. DISCUSSION

We have presented the first direct observation that higher-order scaling of the magnetic and Elsässer field fluctuations depends on the angle of the local magnetic field direction to the (radial) flow. In fluctuations with wavevectors parallel to the local magnetic field direction, global scale invariance is a robust feature of inertial range collisionless plasma turbulence in the fast ambient solar wind. This is distinct from the multifractal scaling that is characteristic of neutral fluid turbulence and MHD fluctuations with wavevectors perpendicular to the local field. These properties must be included in any successful theory that attempts to explain inertial range intermittency.

A process that has multifractal properties generates fluctuations through a multiplicative sequence such as an energy cascade of eddies in turbulent flows, while monofractal processes generate fluctuations through additive sequences. Therefore, the solar wind MHD turbulence cascade proceeds from smaller to larger wavenumbers that are mainly perpendicular to the local magnetic field direction. The presence of monoscaling parallel to the local field indicates that the cascade in this direction does not proceed in the well-understood classic fluid turbulence manner. It could be that kinetic physics is important in the parallel cascade even on what is typically considered MHD scales, and thus behavior associated with kinetic range turbulence such as monoscaling (Kiyani et al. 2009) is observed. Alternatively, the monofractal scaling may be evidence for a weak turbulent cascade. This is consistent with incompressible 3D MHD simulations that found weak (rapid) spectral transfer into wavevectors parallel (perpendicular) to the mean magnetic field (Oughton et al. 1994). This can be understood in terms of resonant three-wave interactions (Shebalin et al. 1983). A weak parallel cascade interpretation would also be consistent with several theories and models of collisionless plasma turbulence (Oughton & Matthaeus 2005) such as reduced MHD (e.g., Montgomery 1982), "critical balance" (Goldreich & Sridhar 1995), and gyrokinetics (Schekochihin et al. 2009). However, while our results imply that the parallel and perpendicular wavevector cascades proceed with different physics, further work is required to determine the exact nature of these differences.

The present analysis applies to intermittent turbulence exclusively in fast ambient solar wind, and further investigation is required to determine whether the phenomenology of spatially anisotropic intermittency is universal. Hence, similar studies will be conducted in different solar wind streams and plasma environments, such as planetary shocks and magnetospheres, with the aim of reproducing the current results. In addition, work has already begun on investigating the presence of similar spatial anisotropy in the higher-order multiscale analysis of dissipation range turbulence, where a dominant monoscaling has already been observed (Kiyani et al. 2009).

This research is supported by UK STFC, EPSRC, and EU Turboplasmas project (Marie Curie FP7 PIRSES-2010-269297). The authors acknowledge useful conversations with S. Oughton, W. H. Matthaeus, and M. Wan.

REFERENCES

Acuña, M. H., Curtis, D., Scheifele, J. L., et al. 2008, SSRv, 136, 203
Anselmet, F., Gagne, Y., Hopfinger, E. J., & Antonia, R. A. 1984, JFM, 140, 63
Bruno, R., & Carbone, V. 2013, LRSP, 10, 2
Chapman, S. C., & Hnat, B. 2007, GeoRL, 34, L17103
Frisch, U. 1995, Turbulence (Cambridge: Cambridge Univ. Press)
Frisch, U., Sulem, P.-L., & Nelkin, M. 1978, JFM, 87, 719
Galvin, A. B., Kistler, L. M., Popecki, M. A., et al. 2008, SSRv, 136, 437
Gogoberidze, G., Chapman, S. C., Hnat, B., & Dunlop, M. W. 2012, MNRAS, 426, 591
Goldreich, P., & Sridhar, S. 1995, ApJ, 438, 763
Greco, A., Valentini, F., Servidio, S., & Matthaeus, W. H. 2012, PhRvE, 86, 066405
Haynes, C. T., Burgess, D., & Camporeale, E. 2014, ApJ, 783, 38
Horbury, T. S., Forman, M. A., & Oughton, S. 2005, PPCF, 47, B703
Horbury, T. S., Forman, M., & Oughton, S. 2008, PhRvL, 101, 175005
Karimabadi, H., Roytershteyn, V., Wan, M., et al. 2013, PhPl, 20, 012303
Kiyani, K. H., Chapman, S. C., & Hnat, B. 2006, PhRvE, 74, 051122
Kiyani, K. H., Chapman, S. C., Khotyaintsev, Yu. V., Dunlop, M. W., & Sahraoui, F. 2009, PhRvL, 103, 075006
Kiyani, K. H., Chapman, S. C., Sahraoui, F., et al. 2013, ApJ, 763, 10
Kolmogorov, A. N. 1962, JFM, 13, 82
Leonardis, E., Chapman, S. C., Daughton, W., Roytershteyn, V., & Karimabadi, H. 2013, PhRvL, 110, 205002
Luhmann, J. G., Curtis, D. W., Schroeder, P., et al. 2008, SSRv, 136, 117
Matthaeus, W. H., Goldstein, M. L., & Roberts, D. A. 1990, JGR, 95, 20673
Matthaeus, W. H., Servidio, S., Dmitruk, P., et al. 2012, ApJ, 750, 103
Monin, A., & Yaglom, A. 1975, Statistical Fluid Mechanics: Mechanics of Turbulence, Vol. 2 (Cambridge, MA: MIT Press)
Montgomery, D. C. 1982, PhST, 2/1, 83
Oboukhov, A. M. 1962, JFM, 13, 77
Osman, K. T., & Horbury, T. S. 2007, ApJL, 654, L103
Osman, K. T., & Horbury, T. S. 2009a, JGR, 114, A06103
Osman, K. T., & Horbury, T. S. 2009b, AnGeo, 27, 3019
Osman, K. T., Matthaeus, W. H., Greco, A., & Servidio, S. 2011a, ApJL, 727, L11
Osman, K. T., Matthaeus, W. H., Hnat, B., & Chapman, S. C. 2012a, PhRvL, 108, 261103
Osman, K. T., Matthaeus, W. H., Wan, M., & Rappazzo, A. F. 2012b, PhRvL, 108, 261102
Osman, K. T., Wan, M., Matthaeus, W. H., Weygand, J. M., & Dasso, S. 2011b, PhRvL, 107, 165001
Oughton, S., & Matthaeus, W. H. 2005, NPGeo, 12, 299
Oughton, S., Priest, E. R., & Matthaeus, W. H. 1994, JFM, 280, 95
Perrone, D., Valentini, F., Servidio, S., Dalena, S., & Veltri, P. 2013, ApJ, 762, 99
Podesta, J. J. 2009, ApJ, 698, 986
Politano, H., & Pouquet, A. 1995, PhRvE, 52, 636
Ruffolo, D., Matthaeus, W. H., & Chuychai, P. 2003, ApJL, 597, L169
Schekochihin, A. A., Cowley, S. C., Dorland, W., et al. 2009, ApJS, 182, 310
Servidio, S., Greco, A., Matthaeus, W. H., Osman, K. T., & Dmitruk, P. 2011, JGR, 116, A09102
Servidio, S., Valentini, F., Califano, F., & Veltri, P. 2012, PhRvL, 108, 045001
She, Z.-S., & Leveque, E. 1994, PhRvL, 72, 336
Shebalin, J. V., Matthaeus, W. H., & Montgomery, D. 1983, JPlPh, 29, 525
Sorriso-Valvo, L., Carbone, V., & Veltri, P. 1999, GeoRL, 26, 1801
Sreenivasan, K. R., & Antonia, R. A. 1997, AnRFM, 29, 435
Taylor, G. I. 1938, RSPSA, 164, 476
TenBarge, J. M., & Howes, G. G. 2013, ApJL, 771, L27
Tessein, J. A., Matthaeus, W. H., Wan, M., et al. 2013, ApJL, 776, L8
Wan, M., Matthaeus, W. H., Karimabadi, H., et al. 2012, PhRvL, 109, 195001
Wu, P., Perri, S., Osman, K., et al. 2013, ApJL, 763, L30